

[advances.sciencemag.org/cgi/content/full/7/25/eabg0377/DC1](https://advances.sciencemag.org/cgi/content/full/7/25/eabg0377/DC1)

## Supplementary Materials for

### **Transformation between elastic dipoles, quadrupoles, octupoles, and hexadecapoles driven by surfactant self-assembly in nematic emulsion**

Bohdan Senyuk, Ali Mozaffari, Kevin Crust, Rui Zhang, Juan J. de Pablo\*, Ivan I. Smalyukh\*

\*Corresponding author. Email: [depablo@uchicago.edu](mailto:depablo@uchicago.edu) (J.J.d.P.); [ivan.smalyukh@colorado.edu](mailto:ivan.smalyukh@colorado.edu) (I.I.S.)

Published 18 June 2021, *Sci. Adv.* **7**, eabg0377 (2021)  
DOI: 10.1126/sciadv.abg0377

#### **The PDF file includes:**

Figs. S1 to S3  
Legends for movies S1 to S5

#### **Other Supplementary Material for this manuscript includes the following:**

(available at [advances.sciencemag.org/cgi/content/full/7/25/eabg0377/DC1](https://advances.sciencemag.org/cgi/content/full/7/25/eabg0377/DC1))

Movies S1 to S5

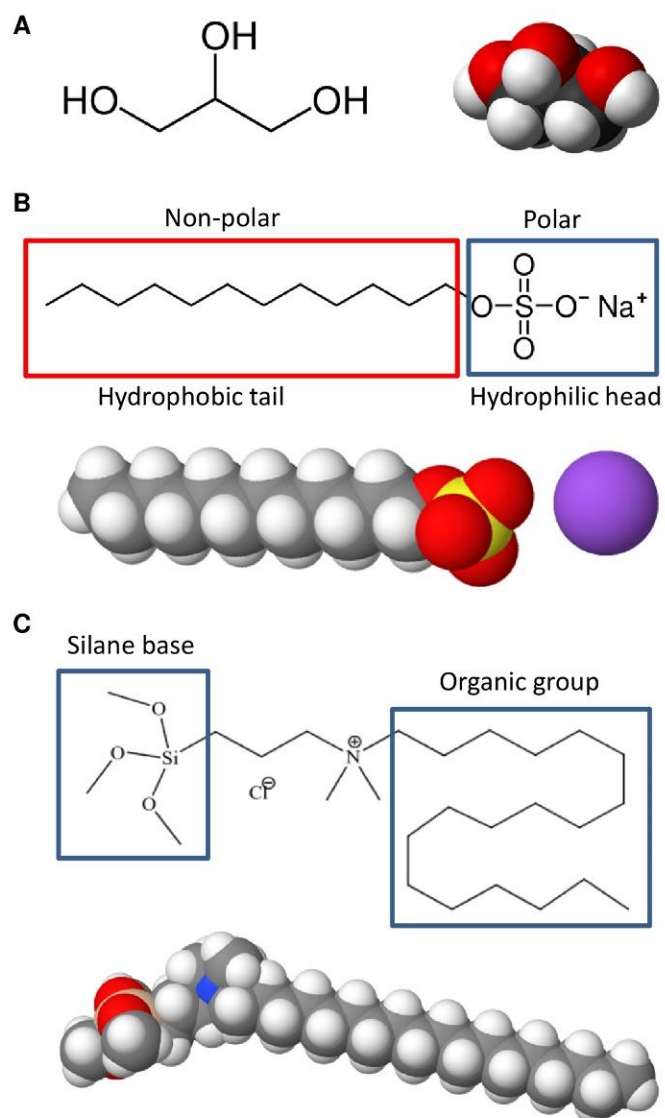


**Fig. S1.** Composition of droplets: (A) Glycerol; (B) Sodium dodecyl sulfate (SDS); (C) N,N-dimethyl-N-octadecyl-3-aminopropyl-trimethoxysilyl chloride (DMOAP).

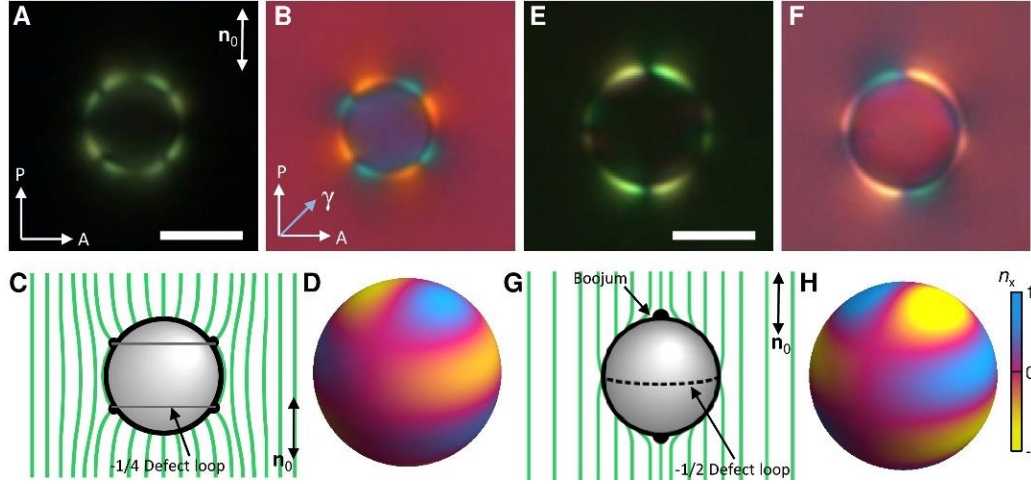


**Fig. S2.** Comparison of the elastic hexadecapoles with (A-D) mixed planar-homeotropic and (E-H) conically degenerate surface anchoring. Scale bars, 5  $\mu\text{m}$ .

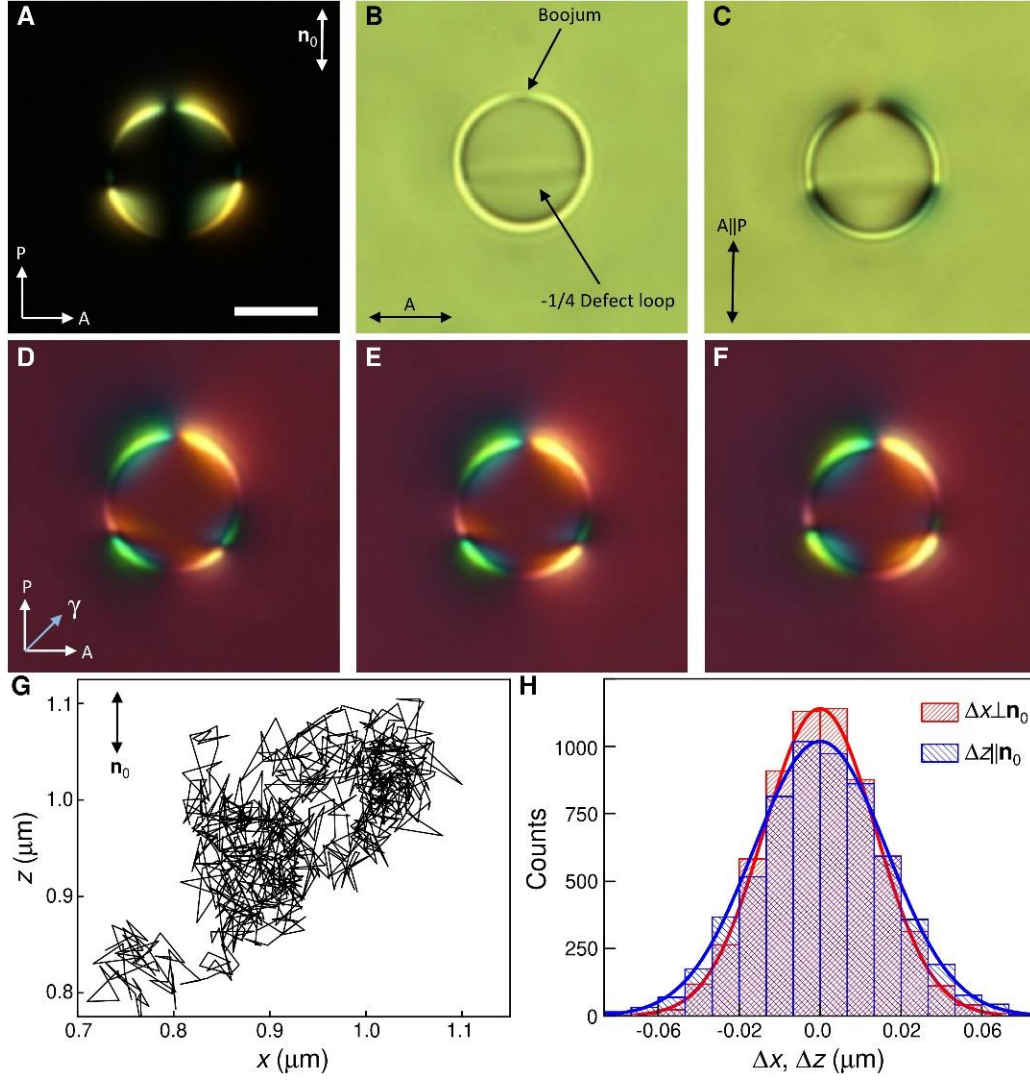


**Fig. S3.** Elastic octupoles and their Brownian motion: (A-F) Optical micrographs between crossed polarizers (A, D-F) without (A) and with (D-F) a retardation plate and between parallel polarizers (C) and without a polarizer (B). (G) Trajectory of the octupole's Brownian motion obtained at a frame rate of 15 fps. (H) Histogram of octupole's displacements with respect to  $\mathbf{n}_0$ . Scale bars, 5  $\mu\text{m}$ .

**Movie S1.**

Optical microscopy textures during a transition from a boojum quadrupole to hedgehog dipole. Timer shows the elapsed time of transformations. P and A mark crossed polarizer and analyzer and  $\mathbf{n}_0$  is a far-field director.

**Movie S2.**

Computer simulations of a transition from a boojum quadrupole to Saturn ring quadrupole: (A) director field configurations with red regions showing the reduced scalar order parameter  $S = 0.3$ ; (B) elastic multipoles shown as a color map of the director's  $x$ -component ( $n_x$ ) on the shell enclosing the droplet and defects. The radius of a mapping shell is  $1.2r_0$ ; (C) polarizing microscopy textures; P and A mark crossed polarizer and analyzer and  $\mathbf{n}_0$  is a far-field director.

**Movie S3.**

Computer simulations of a transition from a boojum quadrupole to octupole: (A) director field configurations with red regions showing the reduced scalar order parameter  $S = 0.3$ ; (B) elastic multipoles shown as a color map of the director's  $x$ -component ( $n_x$ ) on the shell enclosing the droplet and defects. The radius of a mapping shell is  $1.2r_0$ ; (C) polarizing microscopy textures; P and A mark crossed polarizer and analyzer and  $\mathbf{n}_0$  is a far-field director.

**Movie S4.**

Computer simulations of a transition from a dipole to a boojum quadrupole: (A) director field configurations with red regions showing the reduced scalar order parameter  $S = 0.3$ ; (B) elastic multipoles shown as a color map of the director's  $x$ -component ( $n_x$ ) on the shell enclosing the droplet and defects; (C) polarizing microscopy textures; P and A mark crossed polarizer and analyzer and  $\mathbf{n}_0$  is a far-field director.

**Movie S5.**

Computer simulations of a director field change during a transformation of a defect loop into a boojum and the subsequent formation of a semi-ring of disclination corresponding to the boojum core. A red isosurface depicts a region with the reduced scalar order parameter  $S = 0.3$ .